4 An Introduction to the Hubbard Hamiltonian

Richard T. Scalettar
Department of Physics
University of California, Davis

Contents

E. Pavarini, E. Koch, J. van den Brink, and G. Sawatzky (eds.)
Quantum Materials: Experiments and Theory
Modeling and Simulation Vol. 6
Forschungszentrum Jülich, 2016, ISBN 978-3-95806-159-0
http://www.cond-mat.de/events/correl16

1 Introduction

The Hubbard Hamiltonian (HH) offers one of the most simple ways to get insight into how the interactions between electrons give rise to insulating, magnetic, and even novel superconducting effects in a solid. It was written down [1–4] in the early 1960's and initially applied to the behavior of the transition-metal monoxides (FeO, NiO, CoO), compounds which are antiferromagnetic insulators, yet had been predicted to be metallic by methods which treat strong interactions less carefully.

Over the intervening years, the HH has been applied to many systems, from 'heavy fermions' and the Cerium volume collapse transition in the 1980's, to high temperature superconductors in the 1990's. Indeed, it is an amazing feature of the HH that, despite its simplicity, its exhibits behavior relevant to many of the most subtle and beautiful properties of solid state systems. We focus here for the most part on the single-band HH. Multi-band variants like the Periodic Anderson Model (PAM) allow one to introduce other fundamental concepts in many-body physics, such as the competition between magnetic order and singlet formation. Randomness can be simply introduced into the HH, so it can be used as a starting point for investigations of the interplay of interactions and disorder in metal-insulator transitions and, recently, many-body localization. 'Textbook' discussions of the HH can be found in Refs. [5–8] and a recent celebration of its 50th anniversary [9] emphasizes the resurgence of interest due to optical lattice emulation experiments.

The HH has been studied by the full range of analytic techniques developed by the condensed-matter community, from static mean-field approaches (which we will outline here) and the much richer dynamical mean-field theory, to diagrammatic approaches of various degrees of sophistication (the random phase approximation and parquet approach), as well as expansions in the degeneracy of the number of 'flavors' (spin, orbital angular momentum). It has also been extensively attacked with numerical methods like exact diagonalization (ED) and quantum Monte Carlo (QMC).

The objective of these notes is to provide an introduction to the HH and to a few of the most simple ways in which it is solved. Along the way we will discover that these basic calculations lend initial insight to concepts like the Mott gap, moment formation, the mapping of the HH to the Heisenberg model, and magnetism. We begin with a discussion of the second quantized operators with which the HH is written.

2 Creation and destruction operators

Creation and destruction operators $a^\dagger, a$ are familiar from the treatment of the harmonic oscillator. We briefly review their properties, which parallel those of the operators in the HH.

The harmonic oscillator creation and destruction operators are defined in terms of the position and momentum operators,

$$\hat{a} \ = \sqrt{\frac{m\omega}{2\hbar}}\ \hat{x} + i\sqrt{\frac{1}{2m\omega\hbar}}\ \hat{p} \quad \text{and} \quad \hat{a}^\dagger = \sqrt{\frac{m\omega}{2\hbar}}\ \hat{x} - i\sqrt{\frac{1}{2m\omega\hbar}}\ \hat{p}\ . \tag{1}$$

From $[\hat{p}, \hat{x}] = -i\hbar$, one shows that these operators obey the commutation relations,

$$[\hat{a}, \hat{a}^\dagger] = 1 \tag{2}$$

and that the Hamiltonian is,

$$\hat{H} = \frac{1}{2m}\,\hat{p}^2 + \frac{1}{2}m\omega^2\,\hat{x}^2 = \hbar\omega\left(\hat{a}^\dagger\hat{a} + \frac{1}{2}\right). \tag{3}$$

The 'number operator' is defined to be $\hat{n} = \hat{a}^\dagger\,\hat{a}$, so that $\hat{H} = \hbar\omega\,(\,\hat{n} + \frac{1}{2}\,)$.
The ground state of the quantum oscillator is written as $|\,0\,\rangle$ and has the properties that,

$$\hat{a}|\,0\,\rangle = 0 \quad \text{and} \quad \hat{H}|\,0\,\rangle = \frac{\hbar\omega}{2}\,|\,0\,\rangle. \tag{4}$$

The excited states are built up by applying the creation operator repeatedly to the ground state.

$$\hat{a}^\dagger|\,n\,\rangle = \sqrt{n+1}\;|\,n+1\,\rangle \tag{5}$$

and obey the formula,

$$\hat{H}|\,n\,\rangle = \hbar\omega\left(n + \frac{1}{2}\right)\;|\,n\,\rangle. \tag{6}$$

The finite temperature expectation value of any quantum mechanical operator $\hat{A}$ is determined by the Hamiltonian, $\langle\,\hat{A}\,\rangle = Z^{-1}\,\mathrm{Tr}[\,\hat{A}\,e^{-\beta\hat{H}}\,]$. It is simple to verify that $\langle\,\hat{n}\,\rangle = 1/(e^{\beta\hbar\omega} - 1)$, the Bose-Einstein distribution function. For this reason, one often refers to $\hat{a}^\dagger$ and $\hat{a}$ as 'boson' creation and destruction operators. Note that henceforth I will be setting $\hbar = 1$. I will also choose Boltzmann's constant $k_{\rm B} = 1$.
The HH is written in terms of 'fermion' creation and destruction operators. These operators differ in several respects from the operators $\hat{a}^\dagger, \hat{a}$ for a single harmonic oscillator. Perhaps most confusing is a conceptual difference: the fermion operators in the HH are not introduced in terms of familiar position and momentum operators. Rather they stand on their own. Feynman, in his Nobel Prize acceptance speech [10] alludes to this abstractness, *"I didn't have the knowledge to understand the way these were defined in the conventional papers because they were expressed at that time in terms of creation and annihilation operators, and so on, which, I had not successfully learned. I remember that when someone had started to teach me about creation and annihilation operators, that this operator creates an electron, I said, 'how do you create an electron? It disagrees with the conservation of charge', and in that way, I blocked my mind from learning a very practical scheme of calculation"* As in many cases, the passage of time has led to contemptuous familiarity, so that we forget these were once mysterious objects. In addition to the fact they are not written in terms of $\hat{x}$ and $\hat{p}$, another new feature is that in the HH there is a set of creation and destruction operators, which are distinguished by attaching a site index $\mathbf{j}$ and a spin index σ. Thus $\hat{c}^\dagger_{\mathbf{j}\sigma}$ ($\hat{c}_{\mathbf{j}\sigma}$) create (destroy) fermions of spin σ on site $\mathbf{j}$.
As a consequence, the occupation number states are no longer characterized by a single number n, as for a single harmonic oscillator, but instead by a collection of occupation numbers $n_{\mathbf{j}\sigma}$. One writes such states as $|\,n_{\mathbf{1}\uparrow}\,n_{\mathbf{2}\uparrow}\,n_{\mathbf{3}\uparrow}\,n_{\mathbf{1}\downarrow}\,n_{\mathbf{2}\downarrow}\,n_{\mathbf{3}\downarrow}\,\ldots\,\rangle$.

Because these operators are meant to describe fermions, in contrast to Eq. (2), they are defined to have certain *anticommutation* relations. (the anticommutator of two operators $\{\hat{A}, \hat{B}\} = \hat{A}\hat{B} + \hat{B}\hat{A}$)

$$\{\hat{c}_{\mathbf{j}\sigma}, \hat{c}^\dagger_{\mathbf{l}\sigma'}\} = \delta_{\mathbf{j},\mathbf{l}}\,\delta_{\sigma,\sigma'} \qquad \{\hat{c}^\dagger_{\mathbf{j}\sigma}, \hat{c}^\dagger_{\mathbf{l}\sigma'}\} = 0 \qquad \{\hat{c}_{\mathbf{j}\sigma}, \hat{c}_{\mathbf{l}\sigma'}\} = 0\,. \tag{7}$$

Like its bosonic counterpart, $c^\dagger_{j\sigma}|\,0\,\rangle = |\,1\,\rangle$ creates a fermion when acting on the vacuum. However, as a consequence of the anticommutation relations, $\hat{c}^\dagger_{\mathbf{j}\sigma}|\,1\,\rangle = \hat{c}^\dagger_{\mathbf{j}\sigma}\hat{c}^\dagger_{\mathbf{j}\sigma}|\,0\rangle = 0$. This is of course the Pauli principle. The maximum occupation of a particular site with a given spin is 1. Besides the Pauli principle, the anticommutation relations also ensure that the particles are fermions, that is, their wave function changes sign when two fermions with different labels are exchanged, $\hat{c}^\dagger_{\mathbf{j}\sigma}\,\hat{c}^\dagger_{\mathbf{l}\sigma} = -\hat{c}^\dagger_{\mathbf{l}\sigma}\,\hat{c}^\dagger_{\mathbf{j}\sigma}$.

These anticommutation relation require we specify a convention for the relation between a state like $|\,1\,0\,1\,0\,0\,\ldots\,\rangle$ and the vacuum state $|\mathrm{vac}\rangle = |\,0\,0\,0\,0\,0\,\ldots\,\rangle$. The two possibilities, $|\,1\,0\,1\,0\,0\,\ldots\rangle = \hat{c}^\dagger_{\mathbf{1}}\,\hat{c}^\dagger_{\mathbf{3}}\,|\mathrm{vac}\rangle$ and $|\,1\,0\,1\,0\,0\,\ldots\rangle = \hat{c}^\dagger_{\mathbf{3}}\,\hat{c}^\dagger_{\mathbf{1}}\,|\mathrm{vac}\rangle$ differ by a sign. Either definition is fine, but in all subsequent manipulations whatever convention was chosen must be followed consistently. We'll see some examples of the importance of this later.

3 The Hubbard Hamiltonian

Having introduced creation and annihilation operators, we can now write down the HH. Its form arises quite naturally from considering how we might simply describe the motion and interactions of electrons in a solid.

First, we need to account for the fact that there is a regular array of nuclear positions, which for simplicity we consider to be fixed. This suggests that we begin with a lattice of atoms (sites) on which the fermions move. Of course, a single *real* atom is already a very complex structure, with *many* different energy levels (orbitals). The HH simplifies the atoms in a solid to a collection of sites each with a single level (orbital). This is a good picture for a solid with just one energy band at the Fermi surface, so that, indeed, only one orbital is relevant.

With this (big!) simplification, the sites of the HH are constrained by the Pauli principle to four configurations: empty, a single up fermion, a single down fermion, or double occupation by a pair of up and down fermions. (Note that in the relatively new field of optical lattice emulation, the two fermionic types are not electrons of spin up and down, but rather fermionic atoms like ^{6}Li with two possible hyperfine states. I will, however, continue to use 'up' and 'down' to refer to the two fermionic types.)

In a solid where electrons can move around, the electrons interact via a screened Coulomb interaction. The biggest interaction will be for two electrons on the same site. The HH stops just there: interactions are modeled by a term which is zero if the site is empty of fermions or has only a single fermion, but has the value U if the site is doubly occupied (necessarily, by the Pauli principle, by fermions of opposite spin). The expression $U n_{\mathbf{j}\uparrow}\, n_{\mathbf{j}\downarrow}$ captures this property. In the simplest HH, there is no interaction $V n_{\mathbf{l}\sigma}\, n_{\mathbf{j}\sigma'}$ between fermions on different sites $\mathbf{l}$ and $\mathbf{j}$, although such terms are included in the 'extended' HH.

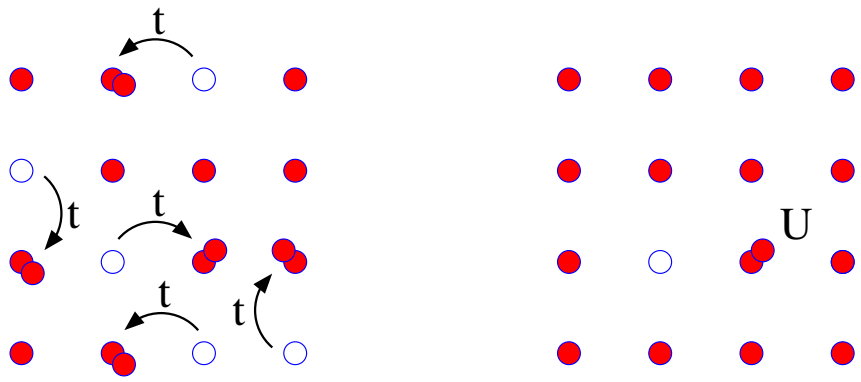

Fig. 1: *Pictorial representation of the terms in the Hubbard Hamiltonian. Left: The kinetic energy t. Right: The on-site repulsion U.*

A reasonable thought for the kinetic energy is an expression which destroys a fermion on one site and creates it on a neighbor. The energy scale t which governs this 'hopping' will be determined by the overlap of two wavefunctions on the pair of atoms. Since wavefunctions die off exponentially, it is reasonable to begin by allowing hopping only between the closest atoms in our lattice.
Formalizing this reasoning, the HH is then, dropping all the 'hats' which had been used to emphasize c , $c^\dagger$ are operators,

$$\hat{H} = -t \sum_{\langle \mathbf{j},\mathbf{l}\rangle\sigma} \left(c^\dagger_{\mathbf{j}\sigma} c_{\mathbf{l}\sigma} + c^\dagger_{\mathbf{l}\sigma} c_{\mathbf{j}\sigma} \right) + U \sum_{\mathbf{j}} n_{\mathbf{j}\uparrow} n_{\mathbf{j}\downarrow} - \mu \sum_{\mathbf{j}} (n_{\mathbf{j}\uparrow} + n_{\mathbf{j}\downarrow}) \,. \tag{8}$$

The first term is the kinetic energy: It describes the destruction of an fermion of spin σ on site $\mathbf{l}$ and its creation on site $\mathbf{j}$ (or *vice-versa*). The symbol $\langle \mathbf{j}, \mathbf{l}\rangle$ emphasizes that hopping is allowed only between two sites which are adjacent. The second term is the interaction energy. It goes through all the sites and adds an energy U if it finds the site is doubly occupied. The final term is a chemical potential which controls the filling. We refer to the situation where there is one fermion per site as 'half-filling' since the lattice contains half as many fermions as the maximum number (two per site). Studies of the HH often focus on the half-filled case because, as we shall see, it exhibits a lot of interesting phenomena (Mott insulating behavior, anti-ferromagnetic order, etc.) The HH is illustrated in Fig. 1.
Before starting to solve the HH in various limits, it is useful to discuss the idea of particle-hole symmetry.

4 Particle-hole symmetry

The Hubbard Hamiltonian has a fascinating 'particle-hole' symmetry (PHS) which allows us to relate its properties for different values of the parameters. PHS is also important because it is the basis of very useful mappings between the attractive and repulsive HH (see Sec. 10), and because it plays a crucial role in QMC simulations.

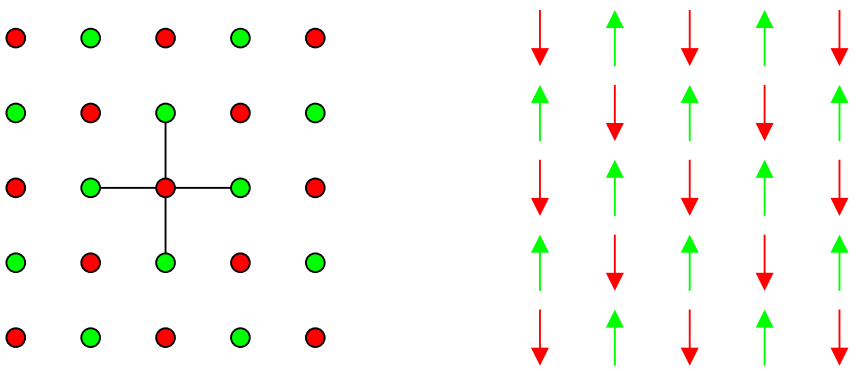

Fig. 2: *Left: The square lattice is bipartite lattice. The near-neighbors of red sites are all green and vice-versa. Right: A bipartite lattice naturally supports antiferromagnetic order in which fermions of one spin are adjacent only to those of opposite spin.*

We first introduce the notion of a bipartite lattice. This is a geometry in which the set of sites can be divided into two *sublattices* $\mathcal{A}$ and $\mathcal{B}$ such that a site in $\mathcal{A}$ has neighbors which are only members of $\mathcal{B}$ and *vice-versa*. See Fig. 2. The square and honeycomb lattices are bipartite, but the triangular lattice is not. Physically, bipartite lattices are highly conducive to antiferromagnetic order, since up and down spin fermions can occupy the two separate sublattices and each spin is always surrounded by neighbors of the opposite spin. Antiferromagnetic order on the triangular lattice is, in contrast, *frustrated*. If each site has a fermion, all conceivable ways to occupy the lattice must possess some bonds connecting sites with spins in the same direction. Bipartite lattices in which the cardinalities of the $\mathcal{A}$ and $\mathcal{B}$ sublattices are different are possible, and, indeed, Lieb has proven some profound theorems concerning ferromagnetism on such lattices. We will encounter these later.

Consider, now, the introduction into the HH of new operators which exchange the role of creation and destruction:

$$d^\dagger_{\mathbf{l}\sigma} = (-1)^{\mathbf{l}} c_{\mathbf{l}\sigma} \, . \tag{9}$$

The $(-1)^{\mathbf{l}}$ factor takes the value -1 on one sublattice and $+1$ on the other. This is aptly named a particle-hole transformation (PHT) because $d^\dagger_{\mathbf{l}\sigma} d_{\mathbf{l}\sigma} = 1 - c^\dagger_{\mathbf{l}\sigma} c_{\mathbf{l}\sigma}$. The occupations (eigenstates of the number operators) $n = 0, 1$ are interchanged.

The key observation is that the kinetic energy in the HH, on a bipartite lattice, is unchanged under a PHT. That is, it takes exactly the same form in terms of the d operators as it did in terms of the c operators:

$$c^\dagger_{\mathbf{l}\sigma} c_{\mathbf{j}\sigma} \quad \rightarrow \quad (-1)^{\mathbf{j}+\mathbf{l}} d_{\mathbf{l}\sigma} d^\dagger_{\mathbf{j}\sigma} \quad = \quad d^\dagger_{\mathbf{l}\sigma} d_{\mathbf{j}\sigma} \, . \tag{10}$$

In obtaining the last equality we used the fact that one minus sign arises from the anticommutation of the two operators, and that a second minus sign arises from the bipartite nature of the lattice, which guarantees that $(-1)^{\mathbf{l}+\mathbf{j}} = -1$.

It is useful to rewrite the HH in a way in which this PHS of the kinetic energy term is present in the interaction term. The expression $U(n_{\mathbf{j}\uparrow} - \frac{1}{2})(n_{\mathbf{j}\downarrow} - \frac{1}{2})$ is also unchanged under the particle-hole transformation. Since $U(n_{\mathbf{j}\uparrow} - \frac{1}{2})(n_{\mathbf{j}\downarrow} - \frac{1}{2}) = U n_{\mathbf{j}\uparrow} n_{\mathbf{j}\downarrow} - \frac{U}{2}(n_{\mathbf{j}\downarrow} + n_{\mathbf{j}\uparrow}) + \frac{U}{4}$, this new form

of the interaction differs from the original only by a trivial shift in the chemical potential and an overall additive constant to the energy.
The upshot is that the PHS form of the HH,

$$H = -t \sum_{\langle \mathbf{j},\mathbf{l}\rangle\sigma} \left(c^\dagger_{\mathbf{j}\sigma} c_{\mathbf{l}\sigma} + c^\dagger_{\mathbf{l}\sigma} c_{\mathbf{j}\sigma} \right) + U \sum_{\mathbf{j}} \left(n_{\mathbf{j}\uparrow} - \frac{1}{2} \right) \left(n_{\mathbf{j}\downarrow} - \frac{1}{2} \right) - \mu \sum_{\mathbf{j}} (n_{\mathbf{j}\uparrow} + n_{\mathbf{j}\downarrow}) \qquad (11)$$

is completely equivalent to the original HH.
The utility of this rewriting is fully appreciated by considering how observables transform. Under a PHT, the density ρ transforms to $1-\rho$, and the HH transforms to the HH with the sign of μ reversed. (The chemical potential term is the only piece of the re-written HH which is not PHS.) As a consequence, $\rho(\mu) = 2 - \rho(-\mu)$ and, in particular, at $\mu = 0$ we have half-filling $\rho = 1$. These statements are true for any value of t, T, or U!
In fact, PHS implies that the whole phase diagram of the HH on a bipartite lattice is symmetric about half-filling. When the square lattice HH is used to model cuprate superconductors, one often includes a next near neighbor hopping t' which connects sites across the diagonal of a square, i.e., sites on the same sublattice. This breaks PHS and the properties of the HH are *not* the same above and below half-filling ($\mu > 0$ and $\mu < 0$), correctly capturing the fact that the hole- and electron-doped cuprates have rather different properties.

5 The single-site limit

Having dealt with this important symmetry, we can get a first insight into the physics of the HH by considering just a single site. Alternately phrased, we can set $t = 0$ in the HH. In this case, $[\hat{H}, n_{\mathbf{j}\sigma}] = 0$ for each $\mathbf{j}$, so that the eigenstates of $\hat{H}$ are also eigenstates of all the *individual* number operators. The number operators also commute with each other, so basic principles of quantum and statistical mechanics tell us we can consider each term in $\hat{H}$ on its own. We thus arrive at a single site model which is very easily solved. (Since all sites are independent, we drop the site index in this limit.)
We have four possibilities corresponding to the site being empty $|\,0\,\rangle$ having a up fermion or down spin fermion $|\uparrow\rangle, |\downarrow\rangle$, or being doubly occupied. $|\uparrow\downarrow\rangle$. Each of these is an eigenstate of $\hat{H}$ with eigenvalues $U/4, -U/4-\mu, -U/4-\mu, U/4-2\mu$, respectively. The partition function,

$$Z = \mathrm{Tr}\left[e^{-\beta \hat{H}} \right] = e^{-\beta U/4} + 2\, e^{-\beta\,(-U/4-\mu)} + e^{-\beta\,(U/4-2\mu)}, \qquad (12)$$

and the occupation is given by,

$$\rho = \langle n_\uparrow + n_\downarrow \rangle = Z^{-1}\, \mathrm{Tr}\left[(n_\uparrow + n_\downarrow)\, e^{-\beta \hat{H}} \right] = Z^{-1} \left(2\, e^{-\beta(-U/4-\mu)} + 2\, e^{-\beta(U/4-2\mu)} \right) \qquad (13)$$

Clearly, $\rho = 1$ at $\mu = 0$ in this expression. But, as emphasized earlier, this is true even at $t \neq 0$. It is instructive to make a plot of ρ vs. μ. Figure 3 shows the result for $U = 4$ and decreasing temperatures $T = 2.0$, 0.5, and 0.25. For $T = 0.25$, *thermal* fluctuations are small and one observes a step-like structure in the density. ρ is small until the chemical potential exceeds

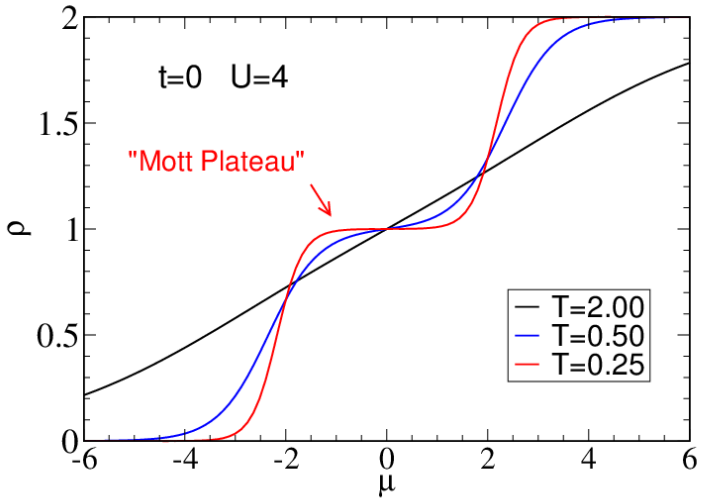

Fig. 3: *Density ρ as a function of chemical potential μ for the single site ($t = 0$) HH. As the temperature decreases, a 'Mott Plateau' develops: Increasing μ initially adds a fermion to the site, but ρ gets frozen at $\rho = 1$. The chemical potential must jump by $\Delta\mu = U$ to add a second fermion. The compressibility $\kappa = \partial\rho/\partial\mu = 0$ in the Mott gap.*

$-U/2$. At this point it rises to $\rho = 1$. However we do not fill the site with a second particle, $\rho = 2$ until μ jumps by U. This is our first encounter with one of the fundamental features of the HH, the 'Mott insulating gap'. This will be discussed in more detail later, but for now we just notice that the presence of one fermion on a site blocks the addition of a second (until a sufficiently large chemical potential overcomes the repulsion). The flat region of $\rho = 1$ extending from $\mu = -U/2$ to $\mu = U/2$ is sometimes referred to as the 'Mott plateau'. The compressibility $\kappa = \partial\rho/\partial\mu = 0$ in the Mott gap.

As seen in Fig. 3, finite temperature T washes out the sharp jumps in ρ. One of the key questions encountered in the HH is to determine the conditions under which *quantum* fluctuations induced by the hopping t destroy the Mott plateau.

A fundamental physical quantity in the HH is the 'local moment'.

$$\langle m^2 \rangle = \langle (n_\uparrow - n_\downarrow)^2 \rangle = \langle n_\uparrow + n_\downarrow \rangle - 2\langle n_\uparrow n_\downarrow \rangle = \rho - 2D \tag{14}$$

where D is the 'double occupancy'. The local moment is zero if the site is either empty ($|\,0\,\rangle$) or has two oppositely pointed spins ($|\uparrow\downarrow\rangle$), but takes the value one if the site has a single fermion ($|\uparrow\rangle$ or $|\downarrow\rangle$).

Figure 4 shows $\langle m^2 \rangle$ as a function of U for fixed $T = 2$ (left), and as a function of T for fixed $U = 4$ (right). The plot shows half-filling $\rho = 1$ ($\mu = 0$). At large U or small T the local moment $\langle m^2 \rangle \to 1$ can become perfectly formed. There is no double occupancy, and hence no empty sites either, if $\rho = 1$. As with the Mott plateau, turning on quantum fluctuations $t \neq 0$ changes the behavior of $\langle m^2 \rangle$. Perfect moments no longer form at $T = 0$ for finite U.

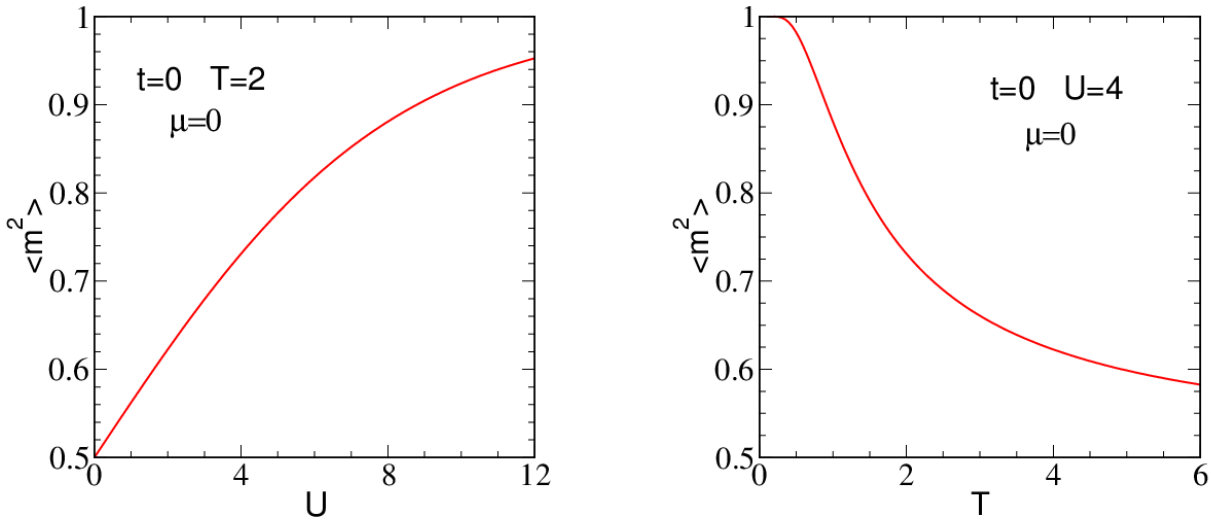

Fig. 4: *Left: The local moment $\langle m^2 \rangle$ as a function of U at fixed temperature $T = 2$. Right: The local moment $\langle m^2 \rangle$ as a function of T at fixed $U = 4$. Local moments develop as either T is reduced or U is increased. Chemical potential $\mu = 0$ in both panels, so the site is half-filled.*

6 The non-interacting Hubbard Hamiltonian

There are two alternate, but equivalent, ways of looking at the $U = 0$ HH. One involves working in real space. The other in momentum space. Let's start with the real space analysis.

We first note that the HH commutes with the operators $N_\uparrow = \sum_{\mathbf{j}} n_{\mathbf{j}\uparrow}$ and $N_\downarrow = \sum_{\mathbf{j}} n_{\mathbf{j}\downarrow}$ which count the *total* number of up and down fermions on the lattice. (There is no commutation with the *individual* number operators as we had for $t = 0$.) You can show this by considering the commutator of the kinetic energy on a single 'link' of the lattice connecting sites $\mathbf{i}$ and $\mathbf{j}$ with the total number of fermions on those two sites, and proving $[c^\dagger_{\mathbf{i}\sigma} c_{\mathbf{j}\sigma} + c^\dagger_{\mathbf{j}\sigma} c_{\mathbf{i}\sigma}, n_{\mathbf{i}\sigma} + n_{\mathbf{j}\sigma}] = 0$. A handy identity in working through the algebra relates commutators and anticommutators, $[AB, C] = A\{B, C\} - \{A, C\}B$. Actually, one can almost guess that this hopping term must conserve particle number, since it contains one creation and one annihilation operator for the relevant sites.

The implication of this commutation is that in finding the eigenstates of the HH, we can consider different sectors of total $N_\uparrow$ and $N_\downarrow$ separately. (This is true even if U is nonzero.) So let's think about the sector where $N_\uparrow = 1$ and $N_\downarrow = 0$. A basis consists of occupation number states $|1\,0\,0\,0\,0\,0\cdots\rangle$, $|0\,1\,0\,0\,0\,0\cdots\rangle$, $|0\,0\,1\,0\,0\,0\cdots\rangle$, ... There are N of these basis vectors, where N equals the number of sites in the lattice. Obviously, we only need to track the up-spin fermion location. Let's imagine for simplicity that we are in one dimension. Applying $\hat{H}$ to these states moves the occupied site to the left or right. As an explicit example for how $\hat{H}$ acts,

$$\hat{H}\,|0\,1\,0\,0\,0\,0\cdots\rangle = -\mu\,|0\,1\,0\,0\,0\,0\cdots\rangle - t\,|1\,0\,0\,0\,0\,0\cdots\rangle - t\,|0\,0\,1\,0\,0\,0\cdots\rangle\,. \qquad (15)$$

Consequentially, the matrix for $\hat{H}$ in this basis is just

$$H = \begin{pmatrix} -\mu & -t & 0 & 0 & \cdots & 0 & -t \\ -t & -\mu & -t & 0 & \cdots & 0 & 0 \\ 0 & -t & -\mu & -t & \cdots & 0 & 0 \\ 0 & 0 & -t & -\mu & \cdots & 0 & 0 \\ \vdots & \vdots & \vdots & \vdots & & \vdots & \vdots \\ -t & 0 & 0 & 0 & \cdots & -t & -\mu \end{pmatrix} . \tag{16}$$

If we impose periodic boundary conditions (pbc) then the first row of the matrix has a $-t$ in its final column, and the last row of the matrix has a $-t$ in its first column, representing a hopping between the first and last sites in the chain.

The eigenvalues of an $N \times N$ tridiagonal matrix with 'a' along the diagonal and 'b' above and below the diagonal, with pbc, are $\lambda_n = a + 2b\cos k_n$ where $k_n = 2\pi n/N$ and $n = 1, 2, 3, \ldots N$. To see this, insert the *ansatz* $v_l = e^{ikl}$ in the eigenvalue equation $a\, v_l + b\, v_{l-1} + b\, v_{l+1} = \lambda\, v_l$. The discretization of k arises from the requirement $v_0 = v_N$ and $v_{N+1} = v_1$, which must be used for the equations with $l = 1$ and $l = N$ to have the above form.

This property of tridiagonal matrices solves the noninteracting HH in the one particle sector for a one dimensional chain. The eigenvalues are $\epsilon(k) = -\mu - 2t\cos k$ and the eigenvector $\vec{v}_k$ has components $(\vec{v}_k)_l = e^{ikl}$. It is interesting to note that, mathematically, this problem is identical to the calculation of the modes of a one dimensional mass-spring system, where the analogous calculation yields the normal modes and (squares of) the normal mode frequencies.

What about the two particle sector? The basis vectors now are the $N(N-1)/2$ occupation number states, $|1\,1\,0\,0\,0\,0\cdots\rangle$, $|1\,0\,1\,0\,0\,0\cdots\rangle$, $|1\,0\,0\,1\,0\,0\cdots\rangle$, $\cdots$. One can take these states and follow the same construction as with $N_\uparrow = 1$: Act with $\hat{H}$ on each one and get the matrix for the HH in this basis. Diagonalizing yields $N(N-1)/2$ eigenvalues and eigenvectors. If you do this, you will find the eigenvalues are just composed of sums of pairs of the eigenvalues of the $N_\uparrow = 1$ matrix, with the 'Pauli Principle' restriction that you choose distinct eigenvalues! This is pretty amazing since, at first glance, the matrices appear completely unrelated to each other. For example, the rows of the matrix for $N_\uparrow = 2$ associated with states in which the occupied sites are not adjacent have four columns with $-t$, while those for states with adjacent occupation have only two columns with $-t$. The matrix looks far less symmetric than for $N_\uparrow = 1$.

Important Note: When you do the calculation you *must* keep very careful track of the signs in returning sequences of creation operators into the order you selected for your convention! Otherwise the eigenvalues for $N_\uparrow = 2$ will *not* be related to those of $N_\uparrow = 1$. See Sec. 2.

The message here is that, in the absence of the interaction term U, all the information about the eigenstates of the HH are contained by solving the single particle sector. However, when $U \neq 0$, the eigenvalues absolutely cannot be obtained in this way. (In fact, you will have to consider the up and down spin fermion occupations together.) Interactions turn the HH into a *many-body problem*.

A second, and much better, way to analyze the $U = 0$ HH is to do a canonical transformation on the creation and destruction operators. Just as in classical mechanics where a canonical

transformation preserves the Poisson brackets, here we seek to preserve the fermion operator anticommutation relations. (The PHT of Sec. 4 has this property.) We define

$$c^\dagger_{\mathbf{k}\sigma} = \frac{1}{\sqrt{N}} \sum_{\mathbf{l}} e^{i\mathbf{k}\cdot\mathbf{l}}\, c^\dagger_{\mathbf{l}\sigma}\,. \tag{17}$$

As already noted above, the momentum $\mathbf{k}$ has discretized values so that there is the same number of momentum creation operators as creation operators in real space.
The following 'orthogonality' identities are very useful

$$\frac{1}{N}\sum_l e^{i(k_n-k_m)l} = \delta_{n,m} \quad \text{and} \quad \frac{1}{N}\sum_n e^{ik_n(l-j)} = \delta_{l,j}\,. \tag{18}$$

They allow you to invert Eq. (17) and prove

$$c^\dagger_{\mathbf{l}\sigma} = \frac{1}{\sqrt{N}} \sum_{\mathbf{k}} e^{-i\mathbf{k}\cdot\mathbf{l}}\, c^\dagger_{\mathbf{k}\sigma}. \tag{19}$$

and also to verify that the anticommutation relations

$$\{c_{\mathbf{k}\sigma}, c^\dagger_{\mathbf{p}\sigma'}\} = \delta_{\mathbf{k},\mathbf{p}}\delta_{\sigma,\sigma'} \qquad \{c^\dagger_{\mathbf{k}\sigma}, c^\dagger_{\mathbf{p}\sigma'}\} = 0 \qquad \{c_{\mathbf{k}\sigma}, c_{\mathbf{p}\sigma'}\} = 0 \tag{20}$$

are indeed preserved by this canonical transformation. The total number operator takes the same form in either basis $\hat{N} = \sum_{\mathbf{j}}(n_{\mathbf{j}\uparrow} + n_{\mathbf{j}\downarrow}) = \sum_{\mathbf{k}}(n_{\mathbf{k}\uparrow} + n_{\mathbf{k}\downarrow})$.
We can also write down the $U = 0$ HH in terms of these momentum space operators.

$$H = \sum_{\mathbf{k}\sigma}(\epsilon_{\mathbf{k}} - \mu)\, c^\dagger_{\mathbf{k}\sigma} c_{\mathbf{k}\sigma} = \sum_{\mathbf{k}\sigma}(\epsilon_{\mathbf{k}} - \mu)\, n_{\mathbf{k}\sigma} \quad \text{with} \quad \epsilon_{\mathbf{k}} = \sum_l e^{i\vec{k}\cdot\vec{a}_l}\,. \tag{21}$$

Here $\vec{a}_l$ are the real space vectors pointing to the nearest neighbors of a given site. (We are assuming t connects only those nearest neighbors.) In one dimension, $\vec{a}_l = \pm\hat{x}$ so that $\epsilon_k = -2t\cos k$, as we have previously observed working in real space. (I have set the lattice constant equal to one.)
This Hamiltonian looks like the one arising in the quantum oscillator in Sec. 2 in the sense that it is expressed in terms of a sum of independent number operators which are all mutually commuting. It is now even more evident that the list of single-particle levels $\epsilon_{\mathbf{k}}$ tells us everything about all the particle sectors: At $U = 0$, even if one has many particles, they just occupy the one particle states in accordance with the Pauli principle.
It is important to realize that the result that an analysis of the one-particle sector gives us full information about the model for any particle number rests only on the fact that the interactions are turned off. It is not necessary that the hopping t between different sites be the same for all pairs of sites, or that it be limited to near neighbors, or that the chemical potential be the same on all sites. All that matters is that $\hat{H}$ be a quadratic form in the fermion creation and destruction operators. To emphasize: To solve any Hamiltonian $\hat{H}$ which takes the form $H = \sum_{\mathbf{l},\mathbf{j}} c^\dagger_{\mathbf{l}}\, h_{\mathbf{l},\mathbf{j}}\, c_{\mathbf{j}}$ with h a (symmetric) matrix of real numbers, simply diagonalize h and allow the resulting energy levels to be filled in a way which satisfies the exclusion principle.

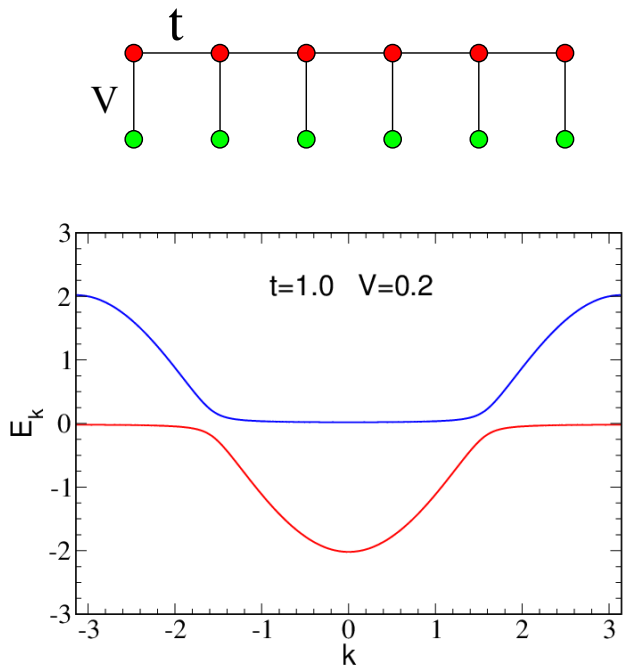

Fig. 5: *Top: The geometry of the PAM in one dimension. Bottom: The dispersion relation.*

We will consider two further examples of computing dispersion relations which illustrate how to handle lattices with a basis ('multiband HH') and also show often encountered geometries. The first adds a 'staggered potential' $\Delta \sum_{\rm l} (-1)^{\rm l} \, n_{\rm l}$ to the HH on a bipartite lattice. Considering, again, a one dimensional chain for simplicity, we write $(-1)^l = e^{il\pi}$. Going to momentum space one encounters,

$$\Delta \sum_l (-1)^l \, c_l^\dagger c_l = \Delta \frac{1}{N} \sum_l e^{i\pi l} \sum_k e^{-ikl} \, c_k^\dagger \sum_p e^{+ipl} \, c_p = \Delta \sum_k c_k^\dagger c_{k+\pi} \tag{22}$$

Going to momentum space has not fully diagonalized the Hamiltonian: the wavevectors k and $k+\pi$ mix. Using the forms already written down for the hopping terms in the HH,

$$H = \sum_k \begin{pmatrix} c_k^\dagger & c_{k+\pi}^\dagger \end{pmatrix} \begin{pmatrix} -2t\cos k & \Delta \\ \Delta & -2t\cos(k+\pi) \end{pmatrix} \begin{pmatrix} c_k \\ c_{k+\pi} \end{pmatrix} \tag{23}$$

where the k sum is over the reduced Brillouin zone $-\pi/2 < k < \pi/2$.

One must still do a final diagonalization of the 2×2 matrices in Eq. (23), which yields the two bands $E_k = \pm\sqrt{(-2t\cos k)^2 + \Delta^2}$. The staggered potential has opened up a band gap at the reduced Brillouin zone boundaries $k = \pm\pi/2$. Understanding the energy bands in a staggered potential is important to doing mean-field theory for the HH. See Sec. 9.

A second example is that of the Periodic Anderson Model (PAM). The PAM is a multi-orbital variant of the HH in which there is a 'conduction' band with creation operators $c_{\rm l}^\dagger$ and a 'localized' band with creation operators $d_{\rm l}^\dagger$. There is no Hubbard U for the conduction band, while

the fermions in the localized band hop only to the conduction band. The Hamiltonian is

$$H = -t \sum_{\langle \mathbf{j},\mathbf{l}\rangle\sigma} \left(c^\dagger_{\mathbf{j}\sigma} c_{\mathbf{l}\sigma} + c^\dagger_{\mathbf{l}\sigma} c_{\mathbf{j}\sigma} \right) + V \sum_{\langle \mathbf{j},\mathbf{l}\rangle\sigma} \left(c^\dagger_{\mathbf{j}\sigma} d_{\mathbf{l}\sigma} + d^\dagger_{\mathbf{l}\sigma} c_{\mathbf{j}\sigma} \right)$$
$$+ U \sum_{\mathbf{j}} \left(n_{d\mathbf{j}\uparrow} - \frac{1}{2} \right) \left(n_{d\mathbf{j}\downarrow} - \frac{1}{2} \right) - \mu \sum_{\mathbf{j}} (n_{c\mathbf{j}\uparrow} + n_{c\mathbf{j}\downarrow} + n_{d\mathbf{j}\uparrow} + n_{d\mathbf{j}\downarrow}) \,. \qquad (24)$$

This geometry is illustrated in one dimension in Fig. 5(top).

Going to momentum space for the non-interacting PAM at $\mu = 0$ yields 2×2 matrices similar in structure to the staggered potential example. We again simplify to one dimension,

$$H = \sum_k \begin{pmatrix} c^\dagger_k & d^\dagger_k \end{pmatrix} \begin{pmatrix} -2t\cos k & V \\ V & 0 \end{pmatrix} \begin{pmatrix} c_k \\ d_k \end{pmatrix} . \qquad (25)$$

A final diagonalization is required to yield the band structure $E_k = \frac{1}{2}\left(\epsilon_k \pm \sqrt{\epsilon_k^2 + 4V^2}\right)$. These two bands exhibit a 'hybridization gap'. Where the dispersionless d-band crosses the c-band at $k = \pm\pi/2$ the hybridization V repels the two curves.

Having computed the dispersion relation $\epsilon_{\mathbf{k}}$, it is valuable to obtain the density of states (DOS)

$$N(E) = \frac{1}{N} \sum_{\mathbf{k}} \delta(E - \epsilon_{\mathbf{k}}) \,. \qquad (26)$$

As its formula makes apparent, the DOS counts the number of energy levels having a particular value E. In the continuum limit (large number of sites), the sum over discrete momenta is replaced by an integral according to the rule $\frac{1}{N}\sum_{\mathbf{k}} \to (2\pi)^{-d} \int d\mathbf{k}$, where d is the spatial dimension. For the one-dimensional HH with $\epsilon_k = -2t\cos k$, $N(E) = 1/(\pi\sqrt{4t^2 - E^2})$. We will use this result in Sec. 9. This DOS diverges at $E = \pm 2t$ where the bands are flat, as we are told should be the case by Ashcroft and Mermin.

A particularly important example of the dispersion relation of the $U = 0$ HH is that of the square lattice, where $\epsilon_{\mathbf{k}} = -2t\,(\cos k_x + \cos k_y)$ according to Eq. (21). One of the reasons this is an interesting geometry is that it forms the simplest picture of the cuprate superconductors: the copper atoms of the CuO_2 sheets reside on a square lattice. Early theories of superconductivity in the cuprates relied on the special van-Hove singularity of the DOS of the square lattice. See Fig. 6(left). One can see the basic idea of the possible role of this divergence from the BCS formula for the superconducting transition temperature $T_c \sim \omega\, e^{-1/VN(E_F)}$. Here V is some coupling constant and ω is an energy scale (a phonon frequency in conventional superconductivity). A large value of the DOS, $N(E_F)$, reduces the size of the negative number in the exponential, boosting T_c. When we discuss Stoner theory we will see another example of how an understanding of the DOS is useful.

Amazingly, the full picture of pairing in the cuprates remains a mystery. The HH is unsolved on the 2D square lattice, and, in particular, whether the ground state away from half-filling has long range d-wave pairing correlations is still open.

As in an electronic structure calculation, the Fermi Surface (FS) of the HH is constructed from the dispersion relation $\epsilon_{\mathbf{k}}$ as the locus of momentum space points that separates filled and empty

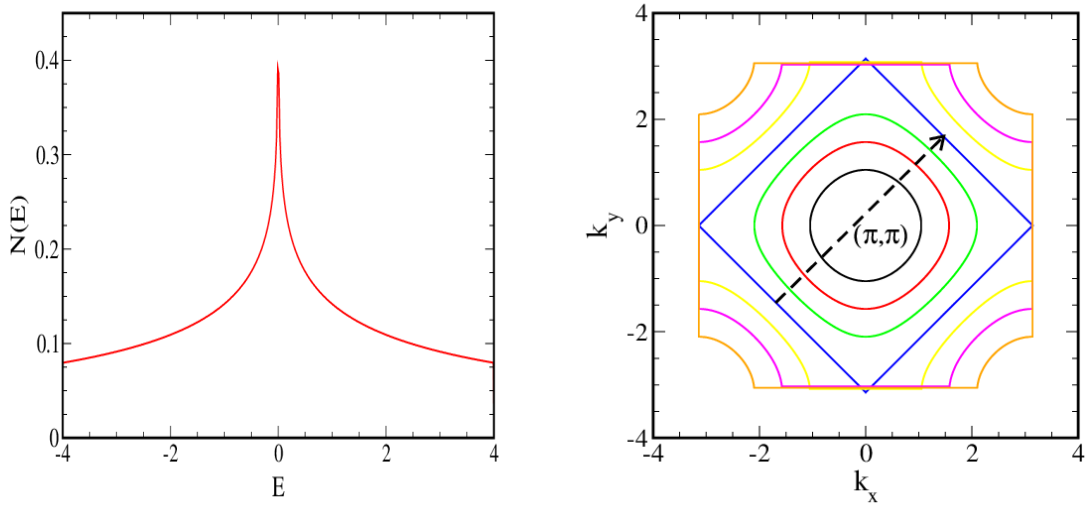

Fig. 6: *Left: The density of states of the square lattice HH. It has a singularity at $\mu = 0$ (half-filling). Right: The Fermi Surface of the square lattice HH for different values of the filling. It evolves from circles about the Γ point at low filling to a rotated square at half-filling $\rho = 1$.*

states at $T = 0$ in the absence of interactions. The FS of the square lattice HH is shown for various values of μ in Fig. 6(right). Like the DOS, the FS of the square lattice has a unique feature at half-filling: perfect nesting. What this means is that the same wave vector $\mathbf{k} = (\pi, \pi)$ maps large segments of the FS onto itself. Since the properties of a fermionic system are dominated by the FS, this suggests that this momentum vector might play a crucial role in the physics of the square lattice. Sure enough, antiferromagnetic order, a large magnetic structure factor at $\mathbf{k} = (\pi, \pi)$, is a feature of the HH at $\rho = 1$ all the way down to $U = 0$.

With $\epsilon_{\mathbf{k}}$ in hand, one can compute all the standard statistical mechanics properties: The partition function, density, internal energy, free energy, and entropy of the $U = 0$ HH are

$$
\begin{aligned}
Z &= \mathrm{Tr}\left[e^{-\beta \hat{H}} \right] = \prod_{\mathbf{k}} \sum_{n_{\mathbf{k}}=0,1} e^{-\beta(n_{\mathbf{k}}-\mu)} = \prod_{\mathbf{k}} \left(1 + e^{-\beta(\epsilon_{\mathbf{k}}-\mu)}\right) \\
\rho &= Z^{-1}\, \mathrm{Tr}\left[\sum_{\mathbf{k}} n_{\mathbf{k}} e^{-\beta \hat{H}} \right] = \sum_{\mathbf{k}} \left(1 + e^{+\beta(\epsilon_{\mathbf{k}}-\mu)}\right)^{-1} = \sum_{\mathbf{k}} f_{\mathbf{k}} \\
E &= Z^{-1}\, \mathrm{Tr}\left[\hat{H}\, e^{-\beta \hat{H}} \right] = \sum_{\mathbf{k}} \epsilon_{\mathbf{k}} \left(1 + e^{+\beta(\epsilon_{\mathbf{k}}-\mu)}\right)^{-1} = \sum_{\mathbf{k}} \epsilon_{\mathbf{k}} f_{\mathbf{k}} \\
S &= \beta\,(E - F) = \beta\, E - \ln Z\ .
\end{aligned}
\tag{27}
$$

Here we introduced the usual definition of the Fermi function $f_{\mathbf{k}}$.

There are several other lattice structures on which the HH is commonly studied and hence whose dispersion relations and DOS are worth knowing. The DOS of the triangular and honeycomb lattices are shown in Fig. 7. The honeycomb lattice is notable for its linearly vanishing DOS at half-filling. Comparison of the DOS of the triangular lattice with that of the square and honeycomb lattices emphasizes the fact that $N(E) = N(-E)$ for bipartite lattices, but not for non-bipartite ones.

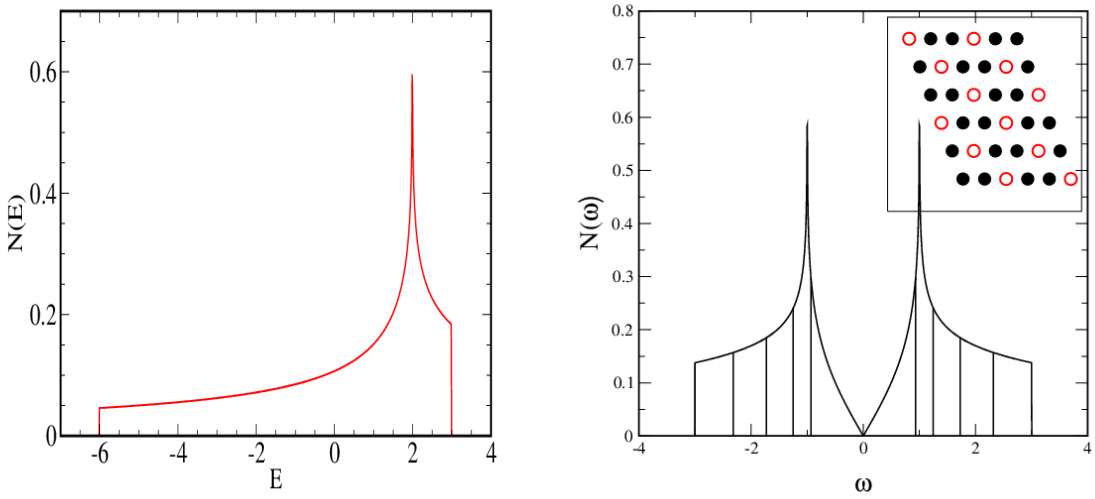

Fig. 7: *Left: The DOS of the $U = 0$ triangular lattice HH. This non-bipartite lattice does not have the property $N(E) = N(-E)$ of the square and honeycomb lattices. Right: The DOS of the $U = 0$ honeycomb lattice HH. Vertical lines demark the chemical potentials of fillings $\rho = 0.1, 0.2, 0.3, \cdots$. Filling $\rho = 0.5$ is at $E = 0$. Inset emphasizes the honeycomb lattice can be viewed as a depleted triangular lattice.*

Our final example is the 'Lieb lattice'. This geometry consists of a square array of sites to which are added additional sites at the midpoint of each bond. See Fig. 8. This structure is of fundamental importance to the cuprate superconductors since it provides a more refined picture of the CuO_2 planes which includes the bridging oxygen sites in addition to the square lattice copper ones. In that application, the parent compounds like La_2CuO_4 have one fermion per CuO_2 unit cell, and there is an additional site energy on the oxygens such that the fermion resides mostly on the coppers.

In the absence of such a site energy, however, something amazing happens. Despite the fact that all the sites are connected and so, seemingly, a fermion placed locally on the lattice would inevitable spread out to occupy the whole structure, instead there are perfectly localized states in real space! Consider Fig. 8 and the state $|\,\psi\,\rangle = (\,c_1^\dagger - c_2^\dagger + c_3^\dagger - c_4^\dagger\,)\,|\,0\,0\,0\,0\,\cdots 0\,\rangle$. When the $U = \mu = 0$ HH for the Lieb lattice acts on $|\,\psi\,\rangle$ one obtains $\hat{H}|\,\psi\,\rangle = 0$! That is, $|\,\psi\,\rangle$ is an eigenstate of $\hat{H}$ of eigenvalue zero. A fermion created onto this cluster of four sites will remain localized there forever. This is quite a surprise since $\hat{H}$ is translationally invariant and we expect the eigenstates to be spread out.

One can reconcile this expectation by noting that this same construction can be done on any equivalent set of four sites on the lattice, so there is a huge set of states all with the same energy $E = 0$. One can form linear combinations of such states which are extended as in Eq. (17). The resulting momentum space states have an energy bands which is completely dispersionless: $\epsilon_{\mathbf{k}} = 0$ independent of $\mathbf{k}$.

This same result can of course be obtained from the procedure we have outlined earlier. Going

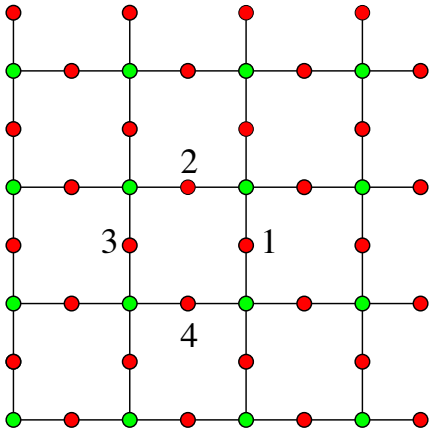

Fig. 8: *The geometry of the 'Lieb lattice'. Creation of a fermion with the appropriate phases on the four labeled sites results in a localized mode. See text.*

to momentum space results in a 3×3 matrix

$$\begin{pmatrix} 0 & -t\,(1+e^{ik_x}) & -t\,(1+e^{ik_y}) \\ -t\,(1+e^{-ik_x}) & 0 & 0 \\ -t\,(1+e^{-ik_y}) & 0 & 0 \end{pmatrix} \tag{28}$$

one of whose energy bands is $E_{\mathbf{k}} = 0$.
Lieb has shown [11] that the presence of such flat bands is a generic feature of bipartite lattices for which the numbers of $\mathcal{A}$ and $\mathcal{B}$ sites are *unequal*. More importantly, ferrimagnetic order can be rigorously proven to occur in the ground state. This is one of the few things known exactly about the HH. We briefly discuss some further interesting interaction-driven physics of the Lieb lattice in Sec. 11.

7 Introduction to exact diagonalization: the two-site HH

The single site HH gave us some insight into the role of U in such phenomena as moment formation and the development of the Mott plateau, but the absence of t precluded any consideration of the interplay between kinetic and potential energy, and the formation of intersite magnetic correlations. These can, however, be captured by examining the HH on two spatial sites. This is the simplest non-trivial example of a powerful method to solve model Hamiltonians: exact diagonalization (ED).
We begin by using the occupation number basis $|\, n_{1\uparrow}\, n_{1\downarrow}\, n_{2\uparrow}\, n_{2\downarrow} \,\rangle$ to enumerate the states in the Hilbert space. The commutation relations $[\hat{H}, n_{1\uparrow} + n_{2\uparrow}] = [\hat{H}, n_{1\downarrow} + n_{2\downarrow}] = 0$ reflect the conservation of the number of up and down fermions, and divide the $2^4 = 16$ states into nine sectors, $(n_{1\uparrow} + n_{2\uparrow}, n_{1\downarrow} + n_{2\downarrow}) = (0,0), (1,0), (2,0), (0,1), (1,1), (2,1), (0,2), (1,2), (2,2)$ of dimensions $1, 2, 1, 2, 4, 2, 1, 2, 1$, respectively. The sectors of dimension 1 immediately identify four eigenstates of the HH on two sites: The completely empty lattice, the lattice completely packed with four fermions, and the states with two like-spin fermions. All these have zero kinetic energy because there are either no fermions present to hop, or else there are two of the

same species and the Pauli principle blocks hopping. The $(2,0)$ and $(0,2)$ energies are $-U/2$ and the $(0,0)$ and $(2,2)$ energies are $+U/2$.

The four sectors of dimension two are almost equally simple. They each have eigenenergies $\pm t$. In the case when there is a single fermion, it can hop between sites. With three fermions, the two which are of like spin are frozen by the Pauli principle and again one has a single fermion which can hop. The fact that the one and three particle sectors have the same spectrum is a reflection of our use of the PHS version of the HH.

The $(1,1)$ sector has dimension four and is the only slightly complicated one. We are rewarded for enduring its diagonalization by some interesting physics. If we denote by $\#$ a site which is doubly occupied, and by 0 a site that is empty, then the action of $\hat{H}$ on the four states $|\uparrow\ \downarrow\rangle, |\downarrow\ \uparrow\rangle, |\#\ 0\rangle, |0\ \#\rangle$, is given by the 4×4 matrix

$$\begin{pmatrix} -U/2 & 0 & -t & -t \\ 0 & -U/2 & -t & -t \\ -t & -t & U/2 & 0 \\ -t & -t & 0 & U/2 \end{pmatrix} . \tag{29}$$

The eigenvalues of this matrix are $-U/2$, $U/2$, $\pm\sqrt{4t^2+U^2/4}$.

We have now discovered the complete spectrum of the two-site Hubbard Hamiltonian. We emphasize again that, in contrast to the noninteracting case $U=0$, we cannot infer all the eigenenergies from consideration of the single particle sector.

The low temperature properties of the two-site HH are determined by the lowest energy eigenstates. These are four of the six states in the half-filled sectors $(2,0),(0,2)$ and $(1,1)$ with energies $-U/2$ (threefold degenerate), $U/2$, and $\pm\sqrt{4t^2+U^2/4}$. If we think about $U \gg t$ we can rewrite $\pm\sqrt{4t^2+U^2/4} = \pm(U/2)\sqrt{1+16t^2/U^2} \approx \pm U/2\,(1+8t^2/U^2) = -U/2 - 4t^2/U,\ +U/2+4t^2/U$.

We have four states with energies roughly $-U/2$ and two with energy roughly $+U/2$. In the thermodynamic limit, these two groupings of states, separated by energy U, are referred to as the 'upper and lower Hubbard bands' (UHB, LHB).

Besides illustrating the UHB and LHB, a particularly nice outcome of this two-site ED analysis is that it also provides a clear illustration of the mapping of the HH to the spin-1/2 Heisenberg model in the large-U limit. It is natural to imagine some such relation between the models because at large U the HH favors single occupation of each site with either an up or a down spin fermion, paralleling the situation of the spin-1/2 Heisenberg model on which each site can have $S_z = \pm 1/2$.

Our solution of the two-site HH allows us to make this mapping more quantitative. Consider two spin-1/2 objects with a Hamiltonian $\hat{H} = J\,\vec{S}_1\cdot\vec{S}_2$. The spectrum is obtained by a trick: $J\vec{S}_1\cdot\vec{S}_2 = J/2\left((\vec{S}_1+\vec{S}_2)^2 - \vec{S}_1^2 - \vec{S}_2^2\right)$. We know $\vec{S}_1^2 = \vec{S}_2^2 = 3/4$ and that, by the rules of adding angular momentum two spin-1/2 combine to spin-0 (non-degenerate 'singlet') or spin-1 (three-fold degenerate 'triplet'). The square of the total spin therefore takes the two values $(\vec{S}_1+\vec{S}_2)^2 = 0, 2$.

This observation allows us to solve the two-site Heisenberg model: $J\vec{S}_1 \cdot \vec{S}_2 = J\,(0 - 3/4 - 3/4) = -3J/4$ or $J\vec{S}_1 \cdot \vec{S}_2 = J\,(2 - 3/4 - 3/4) = +J/4$: The spectrum of the two-site Heisenberg model consists of one state of energy $-3J/4$ and three states of energy $+J/4$.
In the large-U limit, the LHB of the two-site HH has precisely the same structure: a single state of energy $-U/2 - 4t^2/U$ beneath a triplet of states of energy $-U/2$. This makes more precise the qualitative picture discussed above: the eigenspectra are rigorously identical. It also identifies the exchange energy scale $J = 4t^2/U$.
It should be clear that, with the aid of a computer, the ED method can be easily extended to larger numbers of sites [12, 13]. Three functions are at the core of an ED code: The first assigns a basis state number α to each collection of occupation numbers. The second inverts this process, yielding the occupations associated with any basis state number. Finally, a function computes the action of $\hat{H}$ on each basis state $|\alpha\rangle$, using the first function to get the occupations, rearranging the occupations based on the kinetic energy operator, and using the second function to get from these rearranged occupations the states $|\beta\rangle$. For each of these β one sets $H_{\alpha\beta} = \pm t$, where the sign is determined by considering how many interchanges are required to get the operators into their conventional order (as discussed in Sec. 2). The action of the potential energy is easily computed since it does not alter the occupations. Its value is assigned to $H_{\alpha\alpha}$.
More detailed descriptions of the ED method are available in [12,13]. The basic principle really is no more complex than that described above, but as with most simple methods, many clever ideas are involved in pushing them to their limits, such as the use of symmetries to partition $\hat{H}$ into the smallest possible blocks, and, especially, to extract experimentally useful quantities. ED really comes into its own in the computation of dynamical properties, which are very difficult to obtain with competing methods like QMC. For this reason it has been extremely valuable in recent work on thermalization and many-body localization.

8 Green functions: Mott gap and spectral function

As mentioned in the introduction, much of the initial work on the HH involved the use of perturbative, diagrammatic techniques whose central quantities are Green functions G. These approaches, and the important role of G, closely connect with more recently developed QMC methods. For that reason, we will now examine the one-particle Green function in the noninteracting $(U = 0)$ and single site $(t = 0)$ limits. The discussion will also reinforce some of our earlier observations. Much of our discussion will work in real space, since several QMC techniques are formulated there, and our results provide useful context for those methods [14].

8.1 Green functions at $U = 0$

We begin with the definition

$$G_{\mathbf{jn}}(\tau) = \left\langle c_{\mathbf{j}}(\tau) c^{\dagger}_{\mathbf{n}}(0) \right\rangle \quad \text{with} \quad c_{\mathbf{j}}(\tau) = e^{\hat{H}\tau} c_{\mathbf{j}}(0) e^{-\hat{H}\tau}\,. \tag{30}$$

In the limit of no interactions, $G_{\mathbf{jn}}(\tau)$ can be computed analytically. We first note that the imaginary time evolution in momentum space is

$$c_{\mathbf{k}}(\tau) = e^{\hat{H}\tau} c_{\mathbf{k}}(0) e^{-\hat{H}\tau} = e^{-\epsilon_{\mathbf{k}}\tau} c_{\mathbf{k}}(0) \tag{31}$$

This can be verified either by showing that both expressions give the same result on the two states $|\,0\,\rangle$ and $|\,1\,\rangle$, or by using the general theorem that $\partial\hat{A}(\tau)/\partial\tau = [\hat{H}, \hat{A}(\tau)]$.
Transforming the operators in G to momentum space, and using $\langle c_{\mathbf{k}} c_{\mathbf{k}}^\dagger \rangle = 1 - f_{\mathbf{k}}$ we see

$$G_{\mathbf{jn}}(\tau) = \frac{1}{N} \sum_{\mathbf{k}} e^{i\mathbf{k}\cdot(\mathbf{n}-\mathbf{j})} (1 - f_{\mathbf{k}}) e^{-\epsilon_{\mathbf{k}}\tau}. \tag{32}$$

Notice that G is just a function of the difference $\mathbf{n} - \mathbf{j}$, as you would expect for a translationally invariant Hamiltonian.
We have been a little bit careless in defining G. Usually in many-body theory one defines the so-called 'time ordered' Green's function, $G_{\mathbf{k}}(\tau) = -\langle \mathcal{T} c_{\mathbf{k}}(\tau) c_{\mathbf{k}}^\dagger(0) \rangle$ where the time ordering operator T is given by

$$\begin{aligned} \mathcal{T} c_{\mathbf{k}}(\tau) c_{\mathbf{k}}^\dagger(0) &= \quad c_{\mathbf{k}}(\tau) c_{\mathbf{k}}^\dagger(0) \quad \text{for } \tau > 0 \\ \mathcal{T} c_{\mathbf{k}}(\tau) c_{\mathbf{k}}^\dagger(0) &= -c_{\mathbf{k}}^\dagger(0) c_{\mathbf{k}}(\tau) \quad \text{for } \tau < 0\,. \end{aligned} \tag{33}$$

This more precise definition of G leads to the property that $G(\tau+\beta) = -G(\tau)$ for $-\beta < \tau < 0$. Hence the Fourier transform of G

$$G(\tau) = \sum_n G(i\,\omega_n) e^{-i\omega_n\tau} \qquad\qquad G(i\,\omega_n) = \int_0^\beta \frac{d\tau}{\beta} G(\tau) e^{i\,\omega_n\tau} \tag{34}$$

involves the 'Matsubara frequencies' $\omega_n = \pi(2n+1)/\beta$. In momentum space and imaginary time the Green function is given by

$$\begin{aligned} G_{\mathbf{k}}(\tau) &= -e^{-\epsilon_{\mathbf{k}}\tau}(1 - f_{\mathbf{k}}) \quad \text{for} \quad 0 < \tau < \beta \\ G_{\mathbf{k}}(\tau) &= \quad e^{-\epsilon_{\mathbf{k}}\tau} f_{\mathbf{k}} \qquad\quad \text{for} \; -\beta < \tau < 0 \end{aligned} \tag{35}$$

and in momentum space and frequency

$$G_{\mathbf{k}}(i\,\omega_n) = \frac{1}{i\,\omega_n - \epsilon_{\mathbf{k}}}\,. \tag{36}$$

Another way to get this last result is to take $\partial/\partial\tau$ of the definition of the time-ordered Green function written in the form

$$G_{\mathbf{k}}(\tau) = \langle c_{\mathbf{k}}(\tau) c_{\mathbf{k}}(0) \rangle\, \theta(\tau) - \langle c_{\mathbf{k}}(0) c_{\mathbf{k}}(\tau) \rangle\, \theta(-\tau)\,. \tag{37}$$

and then Fourier transform both sides to solve for $G_{\mathbf{k}}(i\,\omega_n)$. This approach is the basis of the 'equation of motion' method for computing G. One starts with the definition of G, takes a time derivative, evaluates the resulting commutators of $\hat{H}$ with the creation operators, and then Fourier transforms. If the Hamiltonian is quadratic in the fermion operators, then the set of equations so obtained closes, even if the different fermion operators mix. Of course, we already knew quadratic Hamiltonians are soluble!

8.2 Green functions at $t = 0$

It is instructive to look at the Green function for a single site, that is, the $t = 0$ HH. We have previously written down the Hilbert space for this problem and obtained the partition function and various equal time quantities. Now consider the calculation of

$$G_\uparrow(\tau) = \langle c_\uparrow(\tau) c_\uparrow^\dagger(0) \rangle. \tag{38}$$

Only the states $|\,0\,0\,\rangle$ and $|\,0\,1\,\rangle$ contribute to the expectation value since the creation operator for up fermions needs to see an empty up state. We compute the action of the sequence of operators on $|\,0\,0\,\rangle$:

$$\begin{aligned} c_\uparrow(\tau) c_\uparrow^\dagger(0)\ |\,0\,0\,\rangle &= e^{H\tau} c_\uparrow(0) e^{-H\tau} c_\uparrow^\dagger(0)\ |\,0\,0\,\rangle = e^{H\tau} c_\uparrow(0) e^{-H\tau}\ |\,1\,0\,\rangle \\ &= e^{H\tau} c_\uparrow(0) e^{+U\tau/4}\ |\,1\,0\,\rangle = e^{H\tau} e^{+U\tau/4}\ |\,0\,0\,\rangle = e^{+U\tau/2}\ |\,0\,0\,\rangle \end{aligned} \tag{39}$$

and similarly for $|\,0\,1\,\rangle$.
Completing the calculation yields

$$G_\uparrow(\tau) = \frac{e^{+\beta U/4} e^{-\tau U/2} + e^{-\beta U/4} e^{\tau U/2}}{2\, e^{\beta U/4} + 2\, e^{-\beta U/4}}. \tag{40}$$

The Green's function is related to the 'spectral density' $A(\omega)$ by

$$G(\tau) = \int_{-\infty}^{+\infty} A(\omega)\, \frac{e^{-\omega\tau}}{e^{-\beta\omega} + 1}\, d\omega\,. \tag{41}$$

One can show that when

$$A(\omega) = \frac{1}{2}\, \big(\, \delta(\omega - U/2) + \delta(\omega + U/2) \,\big) \tag{42}$$

is inserted into Eq. (41), the result of Eq. (40) follows. The spectral function of the one-site HH consists of two delta-function peaks separated by U, a result closely connected to our earlier discussion of the Mott gap. Just as the Mott gap is softened (and perhaps even eliminated) by the introduction of t, the computation of $A(\omega)$ for the full HH is one of the central pursuits of the field.

9 A peek at magnetism

In this section we will discuss three common pictures of magnetism in the HH in order of increasing level of mathematical detail: a perturbation picture of the relative favorability of neighboring fermions being of the same or opposite spin; the Stoner criterion for ferromagnetism; and static mean-field theory (MFT). In the latter case we will only outline the calculation to be done, pointing to the connections with our discussion of the $U = 0$ HH.

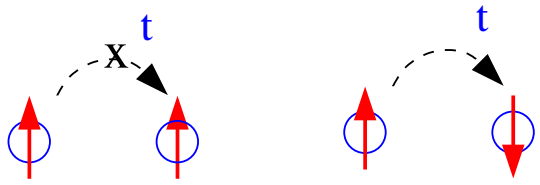

Fig. 9: *The Pauli principle prevents fermions of like spin on adjacent sites from hopping (left), a process which is allowed if the fermions have opposite spin (right).*

9.1 Perturbation theory

We already encountered the 'exchange energy' $J = 4t^2/U$ as the separation between the ground state and the three excited states in the lowest energies of the half-filled sector of the two-site HH. This scale can also be arrived at by doing perturbation theory in t. At $t = 0$, the half-filled HH will have exactly one fermion on every site. Because the sites are independent, the relative orientations are irrelevant to the energy.

Now consider perturbation theory in the hopping. There is no first order shift because the kinetic energy does not connect a state of fixed occupation number with itself. However, there is a second order contribution if the adjacent spins are antiparallel. The kinetic energy $\hat{K}$ can transport a fermion to its neighboring site, resulting in an intermediate state whose doubly occupied site has higher energy $+U$. Then a second action of $\hat{K}$ returns to the original state. The standard perturbation theory formula yields $E^{(2)} \sim -t^2/U$, and a careful counting gives the correct factor of four and $J = -4t^2/U$. This process is forbidden if the two spins are parallel. These two situations are illustrated in Fig. 9.

It is interesting that antiferromagnetism arises both from this strong coupling (perturbation theory in t) argument and also from weak coupling (small U) where we saw the nesting of the Fermi Surface select out the antiferromagnetic wavevector $\vec{k} = (\pi, \pi)$. Indeed, more sophisticated weak coupling approaches like the 'Random Phase Approximation' reinforce the notion that the magnetic susceptibility is largest at (π, π).

9.2 The Stoner criterion

Stoner developed a picture of ferromagnetism based on the competition between the increase in kinetic energy when making the up- and down-spin fermion numbers different and the associated decrease in potential energy. The basic idea is the following: Because of the Pauli principle, the way to occupy a given set of energy levels with the lowest energy is to start filling from the bottom and put two fermions, one of each spin, in each level. Otherwise, if you make the numbers of up and down fermions unequal, and don't fill each level with two fermions, you will have to occupy higher energies.

However, if you make the number of up and down fermions unequal, you can reduce the potential energy: Consider the limit of complete spin polarization where there are no fermions of one spin species. Then, obviously, the potential energy is zero. Very generally, polarization of the spin decreases the likelihood of double occupation and hence lowers the potential energy.

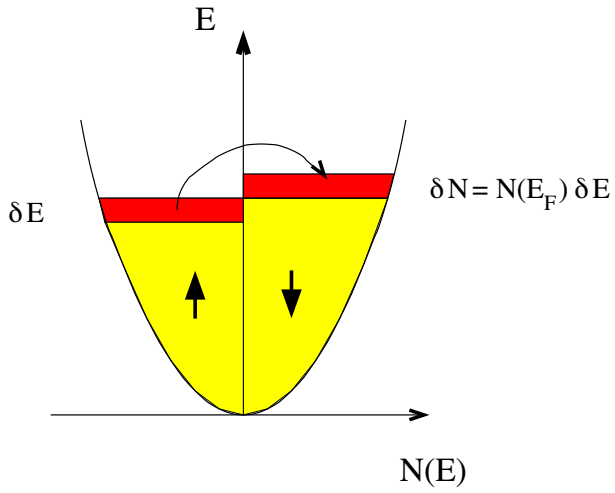

Fig. 10: *Polarizing the fermions increases the kinetic energy, since the levels which must be occupied by the majority species, according to the Pauli principle, are higher than those which could be filled by the minority species.*

Let's now make this argument more precise: Consider a system with density of states $N(E)$ and both up- and down-spin fermions filling the energy levels up to the same maximum Fermi level E_F. The density of up and down fermions is equal. We'll call it n.
We now compute the change in energy which results from a reduction in the density of up-spin fermions by δn and at the same time an increase the number of down-spin fermions by δn. The potential energy is lowered by

$$\delta P = U(n+\delta n)(n-\delta n) - Un^2 = -U(\delta n)^2. \tag{43}$$

If we shift an extra δn fermions into the down group, we will occupy energy levels above the original E_F. Recalling the definition of the density of states as the number of levels at an energy E (see Eq. (26)), we have that $N(E) = \delta N/\delta E$, whence $\delta n = N(E_F)\,\delta E$. This tells us how big the range of energies is above E_F we are filling in terms of δn. Likewise, we are emptying levels below E_F that used to be occupied by up spin fermions. See Fig. 10. The net result of this process is to shift δn fermions up in energy by an amount δE. The change in the kinetic energy is then

$$\delta K = +\delta n \delta E = +\frac{1}{N(E_F)}(\delta n)^2. \tag{44}$$

Putting these two expressions together

$$\delta E = \delta P + \delta K = \left(-U + \frac{1}{N(E_F)}\right)(\delta n)^2 = (-UN(E_F)+1)\,\frac{(\delta n)^2}{N(E_F)}\,. \tag{45}$$

We see that if $UN(E_F) > 1$ the total energy change $\delta E < 0$, so it is favorable to have the up and down fermion densities different and hence favorable to have ferromagnetism. This is called the Stoner criterion. It tells us that magnetism is favored by large fermion interactions and also by large DOS.

9.3 Mean-field theory: the idea and procedure

We have considered the HH in the limits of no hopping ($t = 0$), no interactions ($U = 0$), and small system sizes (one and two sites). We now describe how to use mean-field theory (MFT) to study magnetism.

What is MFT? We commented in an earlier section that a Hamiltonian which is quadratic in the fermion creation and destruction operators, $H = \sum_{\mathbf{l},\mathbf{j}} c^\dagger_{\mathbf{l}}\, h_{\mathbf{l},\mathbf{j}}\, c_{\mathbf{j}}$, can be solved by diagonalizing the matrix h. MFT is a method which produces such a quadratic Hamiltonian from a model like the HH which has quartic terms $U c^\dagger_\uparrow c_\uparrow c^\dagger_\downarrow c_\downarrow$ involving four fermion creation and destruction operators. The approach begins by expressing the number operators as an average value plus a deviation from the average:

$$\begin{aligned} n_{\mathbf{i}\uparrow} &= \langle n_{\mathbf{i}\uparrow}\rangle + (n_{\mathbf{i}\uparrow} - \langle n_{\mathbf{i}\uparrow}\rangle) \\ n_{\mathbf{i}\downarrow} &= \langle n_{\mathbf{i}\downarrow}\rangle + (n_{\mathbf{i}\downarrow} - \langle n_{\mathbf{i}\downarrow}\rangle)\,. \end{aligned} \tag{46}$$

Substituting these expressions into the Hubbard interaction term, and dropping the 'small' term (it's not really small!!) which is the product of the two deviations from the average yields

$$\begin{aligned} n_{\mathbf{i}\uparrow} n_{\mathbf{i}\downarrow} &= [\,\langle n_{\mathbf{i}\uparrow}\rangle + (n_{\mathbf{i}\uparrow} - \langle n_{\mathbf{i}\uparrow}\rangle)\,]\,[\,\langle n_{\mathbf{i}\downarrow}\rangle + (n_{\mathbf{i}\downarrow} - \langle n_{\mathbf{i}\downarrow}\rangle)\,] \\ &\approx \langle n_{\mathbf{i}\uparrow}\rangle\langle n_{\mathbf{i}\downarrow}\rangle + \langle n_{\mathbf{i}\downarrow}\rangle(n_{\mathbf{i}\uparrow} - \langle n_{\mathbf{i}\uparrow}\rangle) + \langle n_{\mathbf{i}\uparrow}\rangle(n_{\mathbf{i}\downarrow} - \langle n_{\mathbf{i}\downarrow}\rangle) \\ &= n_{\mathbf{i}\uparrow}\langle n_{\mathbf{i}\downarrow}\rangle + n_{\mathbf{i}\downarrow}\langle n_{\mathbf{i}\uparrow}\rangle - \langle n_{\mathbf{i}\uparrow}\rangle\langle n_{\mathbf{i}\downarrow}\rangle\,. \end{aligned} \tag{47}$$

The interpretation of this expression is clear. The up-spin fermions interact with the average density of the down-spin fermions, and similarly the down-spin fermions interact with the average density of the up-spin fermions. These two terms overcount the original single interaction term, so the product of the average densities is subtracted off.

Within this mean-field replacement, the Hubbard Hamiltonian is now quadratic, and takes the form (in one dimension)

$$H = -t\sum_{l\sigma}\left(c^\dagger_{l\sigma}c_{l+1\sigma} + c^\dagger_{l+1\sigma}c_{l\sigma}\right) + U\left(\, n_{l\uparrow}\langle n_{l\downarrow}\rangle + n_{l\downarrow}\langle n_{l\uparrow}\rangle) - \langle n_{l\uparrow}\rangle\langle n_{l\downarrow}\rangle\,\right). \tag{48}$$

Since H is quadratic, its solution is a matter of diagonalizing an appropriate matrix. Specifically, for the case of ferromagnetism, one imagines that the average occupation is independent of spatial site $\mathbf{l}$ but allowed to be different for the two spin species. That is, $\langle n_{\mathbf{l}\uparrow}\rangle = n + m$ and $\langle n_{\mathbf{l}\downarrow}\rangle = n - m$. Our goal is to calculate the energy E for fixed n as a function of m and see whether the minimum is at $m = 0$ (paramagnetic state, no ferromagnetism) or $m \neq 0$ (ferromagnetism). Because the expectation values $\langle n_{\mathbf{l}\uparrow}\rangle$ and $\langle n_{\mathbf{l}\downarrow}\rangle$ have a site independent form, the energy levels can easily be written down. (By now we are experts at this!) They are,

$$\epsilon_{\uparrow k} = U(n-m) - 2t\cos k \quad \text{and} \quad \epsilon_{\downarrow k} = U(n+m) - 2t\cos k\,. \tag{49}$$

Again, I have assumed we are in one dimension.

One merely has to take the various possible fillings of the lattice with up and down fermions and add these levels up. That is, we proceed as follows (if doing MFT computationally):

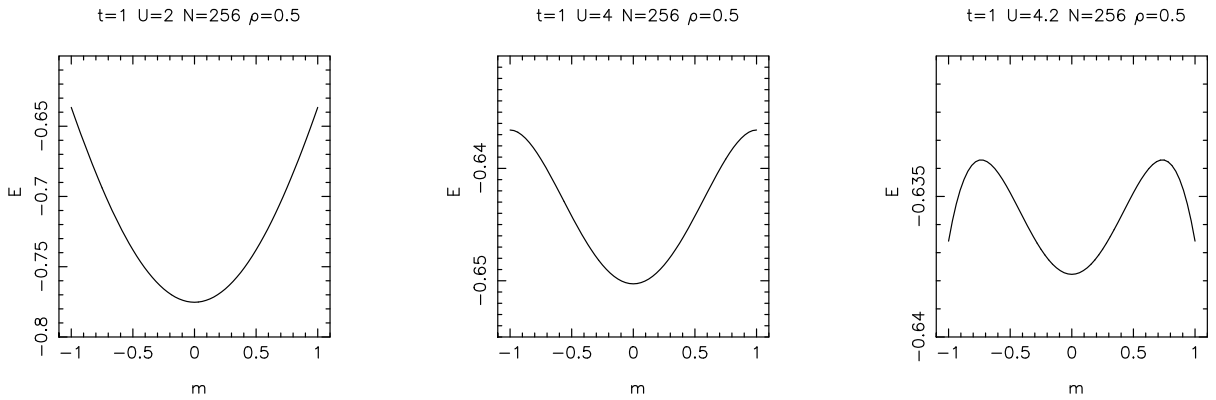

Fig. 11: *Energy versus magnetization of the $d = 1$ HH at $U/t = 2$ and $\rho = \frac{1}{2}$ (quarter filling, 128 fermions on an $N = 256$ site lattice). Left to Right: $U/t = 2.0, 4.0, 4.2$. The minimum energy is always in the paramagnetic phase, $m = 0$. But there is a hint at approaching possibility of ferromagnetism for $U/t = 4.2$ where local minima have begun to develop at $m = \pm 1$.*

(1) Fix the lattice size, N, to some fairly large value, for example $N = 128$ or greater.

(2) Choose a total particle number $N_{\rm tot}$ and on-site repulsion U.

(3) Loop over $N_\uparrow = 0, 1, 2, \ldots, N_{\rm tot}$. For each choice, set $N_\downarrow = N_{\rm tot} - N_\uparrow$. (Actually, your answers should be symmetric on interchange of $N_\uparrow$ and $N_\downarrow$, so you really only need do half the values $N_\uparrow = 0, 1, 2, \ldots, N_{\rm tot}/2$.) Define the densities, $n_\uparrow = N_\uparrow/N$ and $n_\downarrow = N_\downarrow/N$.

(4) Loop over the N allowed momentum values $k = 2\pi/N\{-N/2+1, -N/2+2, \ldots, N/2\}$. Fill up the lowest $N_\uparrow$ and $N_\downarrow$ of the energy levels. Recall that the levels are given by $\epsilon_\uparrow(k) = -2\,t\cos k + U\langle n_\downarrow\rangle$ and $\epsilon_\downarrow(k) = -2\,t\cos k + U\langle n_\uparrow\rangle$.

(5) Finally, normalize the energy to the number of sites and add in the term $-U\langle n_\uparrow\rangle\langle n_\downarrow\rangle$. This gives the energy for the given $N_\uparrow$ and $N_\downarrow = N_{\rm tot} - N_\uparrow$. Make a list of them and see which is lowest.

(6) Repeat the calculation for different U and $N_{\rm tot}$ to get the phase diagram.

9.4 MFT: some results

Figures 11 and 12 give representative results for one quarter filling, that is, a density $\rho = \rho_\uparrow + \rho_\downarrow = \frac{1}{2}$ fermions per site. (This is one quarter of the maximal density of two fermions per site.) The magnetization m is defined such that $m = (\rho_\uparrow - \rho_\downarrow)/(\rho_\uparrow + \rho_\downarrow)$.
At $U/t = 2$ the optimal energy is paramagnetic: the energy E is minimized at $m = 0$. This is still the case at $U/t = 4$, but the energy of the spin polarized solutions (m nonzero) are getting much closer to $m = 0$. (Note the energy scale.) When $U/t = 4.2$ the energies for large $|m|$ have started to turn down and are lower than intermediate m, though $E(m = 0)$ is still lowest. $U/t = 4.4$ has just gone ferromagnetic.

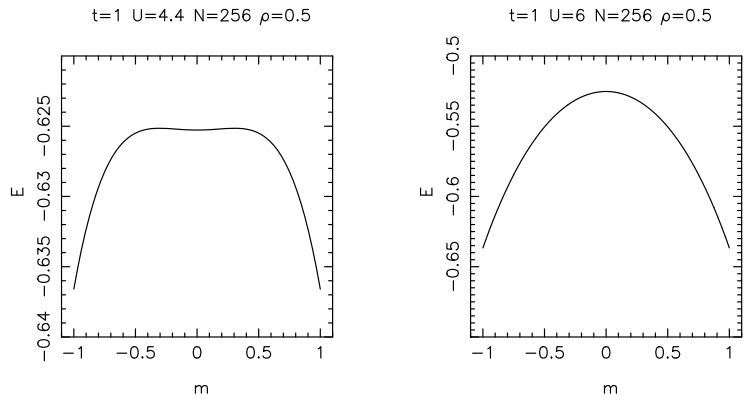

Fig. 12: *Same as Fig. 11 except $U/t = 4.4, 6.0$. The energy minima are now at $m = \pm 1$. The HH has undergone a ferromagnetic phase transition.*

Earlier in this section we derived the Stoner criterion for ferromagnetism, $UN(E_{\rm F}) > 1$. In addition, in Sec. 6, we computed the DOS for the $d = 1$ HH, $N(E) = 1/(\pi\sqrt{4t^2 - E^2})$. (This is the density of states for a single spin species, which is what was used in the Stoner criterion.) To compare with MFT, we need the relation between density ρ and Fermi energy $E_{\rm F}$

$$\rho(E_{\rm F}) = 2\int_{-2t}^{E_{\rm F}} dE\, N(E) \quad \rightsquigarrow \quad \rho_{d=1}(E_{\rm F}) = \frac{2}{\pi}\cos^{-1}\left(\frac{-E_{\rm F}}{2t}\right). \tag{50}$$

We include a factor of two for spin here, so that when we get ρ we use the total density (including both spin species). One can check this latter relation obeys the expected limits: $\rho = 0$ when $E_{\rm F} = -2t$, $\rho = 1$ when $E_{\rm F} = 0$, and $\rho = 2$ when $E_{\rm F} = +2t$.
Putting these equations together, we can get the density of states at $E_{\rm F}$ for a given filling:

$$N(\rho) = \frac{1}{2\pi t}\,\frac{1}{\sin(\pi\rho/2)}\,. \tag{51}$$

For half-filling, $\rho = 1$ we see that $N(\rho = 1) = 1/2\pi t$ and hence $U_{\rm crit} = 2\pi t$. For quarter-filling, $\rho = \frac{1}{2}$ we see that $N(\rho = 1) = 1/\sqrt{2}\pi t$ and hence $U_{\rm crit} = \sqrt{2}\pi t = 4.44t$. This is in pretty good agreement with Figs. 11 and 12 which showed us that $U_{\rm crit}$ was around $4.4t$. The slight disagreement (Fig. 12 suggests $U_{\rm crit}$ a bit less than $4.4t$ while Stoner gives $U_{\rm crit}$ a bit larger than $4.4t$) is a finite size effect. (The calculations were done on an $N = 256$ site lattice.)
One can also do MFT in the grand-canonical ensemble (GCE). That is, rather than computing the energy for fixed occupations, one uses a chemical potential μ and then *computes* $N_\downarrow$ and $N_\uparrow$ by filling those levels which are below μ. The density then comes out of the choice of μ, and, indeed, one needs to tune μ to get the desired density.
One advantage of working in the GCE is that one can frame the calculation in a self-consistent manner, so that starting at some densities $n_\uparrow, n_\downarrow$, the energies are computed and the new values for the densities are inferred, which are fed back into the calculation. The process is iterated until convergence is reached. (There is a danger of getting stuck in metastable configurations, however.)
MFT is an incredibly useful method, and should probably be used as a starting point for understanding almost any new model Hamiltonian. It is, in fact, the technique which was used to

solve the BCS theory of superconductivity: quadratic Hamiltonians can be solved even if they contain 'anomalous' terms consisting of pairs of creation and destruction operators. MFT can also be applied to inhomogeneous problems, for example in a HH with disorder or in situations where inhomogeneities arise spontaneously. It is merely a matter of replacing the analytic forms for the energy bands with a matrix diagonalization. In the former case, some beautiful work has been done on disordered superconductivity. In the latter case, striped phases of the HH were discovered early on via MFT, and seem to play a role in cuprate superconductivity.

9.5 MFT: antiferromagnetism

It should be clear that the basic idea to look for antiferromagnetism in the HH within MFT is the same as for ferromagnetism. Indeed, our earlier solution for the energy bands of the non-interacting HH serves us well here. We simply replace the ferromagnetic ansatz $\langle n_{\mathrm{l}\uparrow}\rangle = n+m$, $\langle n_{\mathrm{l}\downarrow}\rangle = n-m$. by an antiferromagnetic one, $\langle n_{\mathrm{l}\uparrow}\rangle = n+(-1)^{\mathrm{l}}m$, $\langle n_{\mathrm{l}\downarrow}\rangle = n-(-1)^{\mathrm{l}}m$, giving rise to a staggered potential. A bipartite lattice is assumed here.

The process for computing the energy of an antiferromagnetic configuration is the same as the steps (1–5) above, with the replacement of the ferromagnetic eigenvalues by the antiferromagnetic ones. Since we are assuming the total up and down densities over the whole lattice are identical, one no longer loops over different $N_\uparrow$. However, one does have to loop over different m. More precisely, one fixes $n = N_{\mathrm{tot}}/2$ and then tries $m = 1/N, 2/N \ldots$, One also needs to be careful to work in the reduced Brillouin zone.

In concluding this discussion of MFT, it should be emphasized that, while very useful in yielding insight into the possible phases of the system, is a completely uncontrolled approximation. MFT overestimates the tendency for ordered phases, and can (and does) predict magnetic order where none occurs. Even if a particular phase transition is correctly predicted by MFT, the details of the transition (critical temperature, critical exponents, etc) are usually incorrect.

10 The attractive Hubbard Hamiltonian

In Sec. 4 we considered PHTs, which we performed on both spin species. A PHT on only one spin species yields a connection between the HH with $U > 0$ and $U < 0$. In this case, $n_\downarrow \to 1 - n_\downarrow$, but $n_\uparrow \to n_\uparrow$ is unchanged. The kinetic energy term is invariant, but the sign of the interaction term is reversed, $U(n_\uparrow - \frac{1}{2})(n_\downarrow - \frac{1}{2}) \to -U(n_\uparrow - \frac{1}{2})(n_\downarrow - \frac{1}{2})$, and the chemical potential μ maps into a Zeeman field term $-\mu(n_\uparrow - n_\downarrow)$. Conversely, a Zeeman term in the original $U > 0$ model maps into a chemical potential term in the $U < 0$ model.

The HH with $-U$ is called the *attractive* HH because a negative value of U represents an attraction between spin up and spin down fermions on the same site. By considering how this

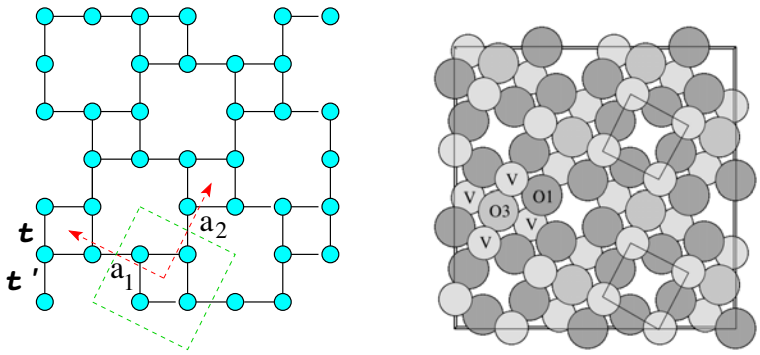

Fig. 13: *The magnetic vanadium atoms of CaV_4O_9 occupy a 1/5 depleted square lattice.*

partial PHT affects various operators, like the components of magnetization,

$$\begin{aligned} S^z_{\mathbf{i}} &= n_{\mathbf{i}\uparrow} - n_{\mathbf{i}\downarrow} \leftrightarrow n_{\mathbf{i}} = n_{\mathbf{i}\uparrow} + n_{\mathbf{i}\downarrow} \\ S^+_{\mathbf{i}} &= c^\dagger_{\mathbf{i}\uparrow} c_{\mathbf{i}\downarrow} \leftrightarrow c^\dagger_{\mathbf{i}\uparrow} c^\dagger_{\mathbf{i}\downarrow} \\ S^-_{\mathbf{i}} &= c^\dagger_{\mathbf{i}\downarrow} c_{\mathbf{i}\uparrow} \leftrightarrow c_{\mathbf{i}\downarrow} c_{\mathbf{i}\uparrow} \end{aligned} \tag{52}$$

one can show that magnetic order in the $+U$ HH is related to superconducting and charge order in the $-U$ HH, so that an understanding of the phases of one model immediately implies considerable information about the other.

For example, imagine starting with the 2D square lattice repulsive HH at half-filling. Its continuous xyz spin rotational invariance precludes long range magnetic order at finite temperature owing to the Mermin-Wagner theorem. (One of the key achievements of QMC was showing that the *ground* state does have order [15].) However, if a Zeeman field is added, this symmetry is reduced to xy, allowing for a Kosterlitz-Thouless transition at $T \neq 0$. Performing the partial PHT we infer that the doped attractive 2D HH (recall the Zeeman field for $U > 0$ maps onto a chemical potential for $U < 0$) has a finite temperature superconducting phase transition. This is a highly non-trivial assertion, made 'obvious' by the PHT. These sorts of considerations can be extended to various exotic sorts of pairing [16].

11 A peek at research: CaV_4O_9

Some of the current research on the HH takes a look at the properties of the HH on 'depleted lattices'. We already encountered one such geometry: the Lieb lattice has a regular array of 1/4 missing sites. As we noted, its band structure possesses a perfectly flat band, and it is interesting to try to understand how this affects magnetism (for $U > 0$) and superconductivity (for $U < 0$) [17]. Lieb [11] has given us some theorems about the former case, although quantitative calculations are still of interest. In the latter case, an intriguing question is the following: Consider the large (attractive) U limit of the HH. Tightly bound fermion pairs can be thought of as bosons, and superconductivity as Bose Einstein Condensation. However, if the band in which the bosons reside is perfectly flat, into which momentum state will they choose to condense?

A second depleted lattice that has been investigated [18] is a model of CaV_4O_9. See Fig. 13. The appropriate HH, or Heisenberg model in the large U limit, has distinct hoppings t and t' within four site plaquettes and between them. It turns out there is a window of $t'/t \approx 1$ (or $J'/J \approx 1$) where long range antiferromagnetic order forms at low temperature. Outside of that window, the ground state is a spin liquid.

12 Conclusions

In these notes we have tried to provide an introduction to the Hubbard Hamiltonian and some of its elementary physics. We have seen how to write the model down and understand its behavior in the limit of no interactions, no kinetic energy, small clusters (ED), and, finally, mean-field theory. We have not discussed the many sophisticated analytic and numerical methods that have been thrown at this simple, but remarkably stubborn, model.

One key piece of physics not addressed here, which arises prominently in the HH, and in its multiband variants like the PAM, is the idea of a 'Kondo resonance'. It turns out that as one progresses from weak to strong coupling, the spectral function does not smoothly evolve from a single blob to two (upper and lower) Hubbard bands. Instead, somewhere in the course of changing the interaction strength a three peak structure is in evidence: The beginning of the formation of upper and lower Hubbard bands, but also a sharp peak at the Fermi energy. This very important idea is at the heart of much of the research into the HH and its experimental realizations, and its successful capture was one of the key achievements of dynamical mean-field theory.

References

[1] M.C. Gutzwiller, Phys. Rev. Lett. **10**, 159 (1963)

[2] J. Kanamori, Prog. Theor. Phys. **30**, 275 (1963)

[3] J. Hubbard, Proc. R. Soc. A **276**, 237 (1963)

[4] J. Hubbard, Proc. R. Soc. A **281**, 401 (1964)

[5] P. Fazekas: *Lecture Notes on Electron Correlation and Magnetism* (World Scientific, Singapore, 1999)

[6] M. Rasetti (ed.): *The Hubbard Model – Recent Results* (World Scientific, Singapore, 1991)

[7] A. Montorsi (ed): *The Hubbard Model – A Reprint Volume* (World Scientific, Singapore, 1992)

[8] F. Gebhard: *The Mott Metal-Insulator Transition, Models and Methods* (Springer, Heidelberg, 1997)

[9] Editorial: *The Hubbard model at half a century*, Nature Physics **9**, 523 (2013)

[10] `http://www.nobelprize.org/nobel_prizes/physics/laureates/1965/feynman-lecture.html`

[11] E.H. Lieb, Phys. Rev. Lett. **62**, 1201 (1989)

[12] N. Laflorencie and D. Poilblanc: *Simulations of pure and doped low-dimensional spin-1/2 gapped systems*, Lecture Notes in Physics **645**, 227 (2004)

[13] `http://wiki.phys.ethz.ch/quantumsimulations/_media/quantumsimulation_ed_part_2.pdf`

[14] R. Blankenbecler, D.J. Scalapino, and R.L. Sugar, Phys. Rev. D **24**, 2278 (1981)

[15] J.E. Hirsch and S. Tang, Phys. Rev. Lett. **62**, 591 (1989)

[16] R.R.P. Singh and R.T. Scalettar, Phys. Rev. Lett. **66**, 3203 (1991)

[17] V.I. Iglovikov, F. Hébert, B. Grémaud, G.G. Batrouni, and R.T. Scalettar, Phys. Rev. B **90**, 094506 (2014)

[18] E. Khatami, R.R.P. Singh, W.E. Pickett, and R.T. Scalettar, Phys. Rev. Lett. **113**, 106402 (2014)